

Lighthweight and heavy-duty instrumented, servo assisted dynamic cone penetrometers for shallow soil characterisation

Miguel Angel Benz Navarrete^{1#}, Pierre Breul², Quoc Anh Tran¹, Caroline Forestti¹
and Tuan Anh Luong^{3,1}

¹*Sol Solution, Research, Innovation and Development department, Riom, France*

²*Institut Pascal, Université Clermont Auvergne, Aubière, France*

³*Gustave Eiffel University, SRO Laboratory, Marne la Vallée, France*

[#]*Corresponding author: mbenz@sol-solution.com*

ABSTRACT

Based on the principle of the Panda® penetrometer, a third-generation of variable-energy dynamic cone penetrometer has been developed in France: the Panda 3⁽¹⁾. This is an instrumented dynamic penetrometer which, by measuring strain, acceleration, and displacement on the rods, close to the anvil, and then decoupling the deformation waves created by the impact and propagating within the rods during penetration, makes it possible to obtain for each blow, at the soil/cone interface, a dynamic load penetration curve, called DCLT curve. Several experimental and numerical studies have been carried out to develop different techniques for processing DCLT curves and dynamic signals to assess input energy, dynamic and pseudo static cone resistance, dynamic stiffness, elastic modulus, and compressional wave velocities of soil. This technique has been adapted to the DPSH cone penetrometer (ISO 22476-2), for which it was necessary to servo-assisted the impact force as a function of the soil penetration obtained after each blow to improve then the quality of the signals and DCLT curves obtained. Recently, in France, a vast experimental program involving two universities and two geotechnical companies was carried out to develop this new technique. A large laboratory and in-situ test data base was performed. After a brief presentation of the theoretical and technological development of this new technique is presented.

Keywords: Soil characterization, Dynamic Penetrometer, Panda 3, Grizzly EV, instrumented DCP, wave equation, DCLT curve, cone loading test.

1. Introduction.

Dynamic Penetration Testing (DPT) is a worldwide soil characterisation technique. It is certainly the oldest in situ geotechnical test, with the first known experience dating back to the 17th century in Germany (Goldmann, 1699). At the beginning of the 20th century, the first major development also took place in Germany with the development of a lightweight dynamic penetrometer, the Künzel Prüfstab, later standardized in 1964 as the "*Light Penetrometer Method*", cf. (Broms & Flodin, 1988).

The principle of the test is simple and due to its rapid implementation, affordability, and suitability for a wide range of soils, DPTs are currently used in geotechnical practice in many countries (Broms & Flodin, 1988; Sabtan & Shehata, 1994; Salgado & Yoon, 2003; Sanglerat, 1972; Scala, 1956; Sowers & Hedges, 1966; Webster et al., 1992). In Europe, their use and characteristics are described in (CEN, 2007; ISO-22476-2, 2005)

However, its technical and technological development have remained in most cases the same as described by N. Goldmann 300 years ago. Furthermore, the interpretation of DPT has remained largely empirical, and the analysis of the penetration phenomenon has always been based on a theoretical principle founded on

Newton's impact theory, which can be challenged for DPTs benefits.

Nowadays, the demand for geotechnical in-situ testing methods is constantly increasing and the development of dynamic penetration tests represents a simple and important means to characterise soils, to study them and to model the spatial variability of their main properties. The aim is to reduce the risks associated with soil uncertainties and hazards, particularly in shallow surface work, and to provide in-situ data to facilitate numerical soil modelling. In addition, we need today to develop cost-effective methods based on simple equipment to study surface soils in large numbers, simply and quickly, and if possible, in an eco-friendly and sustainable way to reduce the impact on the environment (or geotechnical supervised structure).

In the current context, the dynamic penetrometer represents an attractive development opportunity for geotechnical campaigns, provided that:

- Include current technologies in terms of sensors and acquisition chains.
- Develop simple, intelligent, cost-effective robust dynamic penetrometers.
- Develop more efficient signal analysis techniques based on advanced approaches (e.g., transient analysis, wave equation).

- Create and develop laboratory and field databases to facilitate the analysis and interpretation of dynamic penetrometer measurements.
- Develop eco-friendly, sustainable and adaptive processes to conduct tests in the field.
- Identify areas of application where these techniques can complement conventional methods by providing additional data.
- Organize the necessary lobbies to standardize practices and establish specific obligations (*devices characterizes, test procedures, material verification, energy calibration...*) to ensure the quality of data collected in the field using these tools.

With regard to the modernization of the technique, associated technology, and the corresponding theory for analyzing the phenomenon of dynamic penetration in soils, it is noteworthy that over the last 30 years, thanks to the miniaturization of sensors, the widespread availability of computers, increased computing power, the development of numerical methods, and the enhancement of constitutive and engineering soil models, a substantial amount of work has been conducted in the study of dynamic penetrometers.

2. Instrumented dynamic penetrometer.

Because of the rudimentary (and even severe) nature of the test and its mode of operation, which involves large amounts of energy and significant inertial effects, instrumenting dynamic penetrometers is no easy task.

However, theoretical work on driving elongated elastic bars (Barré de Saint-Venant, 1867) such as piles, penetrometers... (Smith, 1960), and the necessity for experimental data to substantiate these theories, have led researchers to instrument bars during the driving process.

In terms of the instrumentation of dynamic penetrometers, it can be noted that a milestone in this field was established through the works of (Fairhurst, 1959) who first instrumented a penetrometer for studying rock percussion in laboratory experiments.

Later, in France (Aussedat, 1970) was truly the first to instrument a dynamic penetrometer to study, in laboratory, soil behaviour by applying the theory of wave propagation. In 1979, (Schmertmann, 1978; Schmertmann & Palacios, 1979) published his work on SPT instrumentation, with the aim of gaining a better understanding of the drive phenomenon and, above all, demonstrating the influence of the energy transmitted on the obtained results. Since then, numerous studies have been carried out on the instrumentation of the SPT dynamic penetrometer.

In 1990, (Gourvès, 1991; Gourvès & Barjot, 1995) in Clermont-Ferrand, France, developed the first instrumented and industrialized dynamic penetrometer. He not only installed sensors to automatically measure and record the driving energy and penetration per blow but also introduced the innovative concept of variable energy drive. Some years later, (Khalaf & Briaud, 1992; Liang & Sheng, 1993) instrumented a penetrometer in the laboratory to obtain wave equation parameters in pile driving problems. (Byun & Lee, 2013; Kianirad, 2011;

Nazarian et al., 1998) and later (Byun & Lee, 2013) instrumented a lightweight dynamic penetrometer to introduce cone index correction by energy transfer and evaluate the soil strength. In Japan, (Matsumoto et al., 2015) instrumented SPT and DPTs to measure energy the drive energy and improve their analysis. Moreover, (DeJong et al., 2017) instrumented the Becker penetrometer, enabling the wave equation to be applied for analysis, thus improving the characterisation of gravelly soils.

However, none of these works has made it possible to improve systematically the technology associated with DPT either to implement new methods of measurements and analysis, or to obtain in situ soil stress and strain necessary for the most current geotechnical problems.

In 2009, in France, based on Panda penetrometer, (Benz et al., 2013; Benz-Navarrete, 2009) developed the first instrumented lightweight variable-energy dynamic penetrometer (The Panda 3®, hereafter iLDCPT) equipped with strain gauges, accelerometers and displacement sensors. This innovation enables the measurement of energy transmitted at each blow and the application of an analysis based on the wave equation to obtain a dynamic load penetration curve (hereafter, DCLT curve) for each impact. More recently, in 2016, (Benz Navarrete et al., 2019; Escobar Valencia et al., 2016) the same principle has been applied to the DPSH penetrometer. In its operating mode, researchers developed an automatic servo-control system to adapt the impact energy based on the soil's hardness, resulting in higher-quality measurements. The first DPSH servo assisted with energy measurement was developed (the Grizzly-3®⁽¹⁾, hereafter iDPSH-EV).

3. Instrumented Lightweight and DPSH cone penetrometers with variable energy driving.

The principle remains the same as that of Panda: drive the penetrometer at variable driving energy and recorded each blow. However, the theoretical basis, instrumentation, and measurement analysis are more sophisticated. (Benz Navarrete et al., 2021) describes the primary fundamental principle of iLDCPT (Panda 3) and iDPSH-EV (Grizzly-3).

3.1. Principle

During the penetration test, and for each blow provided, the sensors installed at the instrumented anvil recorded the strain, acceleration, and displacement. From these recordings, an integrated and automated numerical procedure is used to separate the fundamental descending and ascending waves propagating inside the penetrometer rods (immediately after the hammer blow and for the duration of the cone's penetration into the soil, ~ 50µs) and being the solution of the wave equation. Knowing these waves makes it possible, to compute, by means of reconstruction methods, the stress, strength, velocity, and displacement, as well as the energy transmitted, at cone/soil interface.

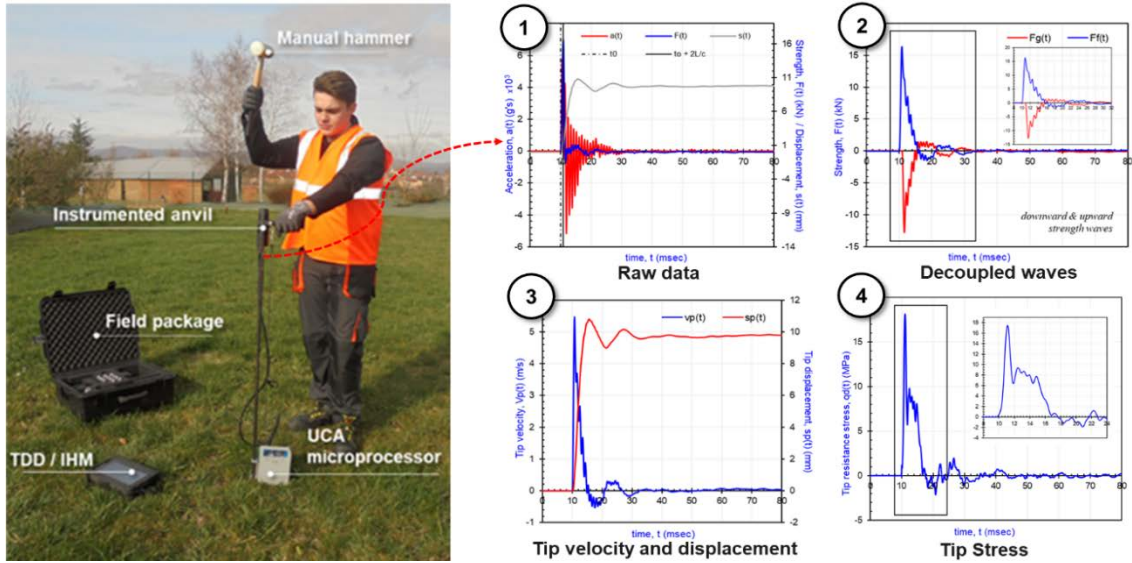


Figure 1. Instrumented lightweight dynamic penetrometer Panda 3 – Main principle. Equipment and instrumentation of iLDCP (Panda 3)

In simplified form, a dynamic cone load-settlement curve (DCLT) is plotted for each blow recorded in depth. From these curves and all the data recorded; various parameters are determined, including dynamic and pseudo-static resistance, dynamic stiffness, shear modulus, shear wave velocity, etc.

3.2. Wave decoupling and cone signal reconstruction

The waves propagating inside the rods are described by the wave equation. To solve it, it is necessary to separate the descending and ascending waves in the recorded acceleration and strain measurements.

In this way, wave decoupling can be performed by different methods. These are distinguished on the types and number of sensors used as well as initial and boundary conditions. In iLDCPT and iDPSH, the method employed is based on a single x_A point measurement, at the instrumented anvil, where strain $\varepsilon_A(t)$ and acceleration $a_A(t)$ are recorded, from which the velocity $v_A(t)$ is calculated. In the point x_A of measurements, the downward $\varepsilon_f(t)$ and upward $\varepsilon_g(t)$ waves are separated by:

$$\begin{aligned} \varepsilon_f(t) &= \frac{1}{2} \left[\varepsilon_A(t) - \frac{v_A(t)}{c_t} \right] \\ \varepsilon_g(t) &= \frac{1}{2} \left[\varepsilon_A(t) + \frac{v_A(t)}{c_t} \right] \end{aligned} \quad (1)$$

Assuming and neglecting the external forces (skin friction, impedances changes...) along the rods, the information about $\varepsilon_f(t)$ and $\varepsilon_g(t)$ allows us to calculate the signals of the force $F_C(t)$ and the velocity $v_C(t)$ for every point C situated under the measurement point A , especially at the cone/soil interface (Eq. 2). In Eq. 2, $\Delta t_{ac} = (x_C - x_A)/c_t$ is the time taken for the waves to travel the distance between the measuring point A on the anvil and the cone/soil interface C .

The displacement $s_C(t)$ is obtained by integration of the signal $v_C(t)$, and energy transmitted to the soil $E_C(t)$, by integrating the product of $F_C(t)$ and $v_C(t)$.

$$\begin{aligned} F_C(t) &= \frac{E_t A_t}{2} [\varepsilon_A(t + \Delta t_{ac}) + \varepsilon_A(t - \Delta t_{ac})] \\ &\quad + \frac{1}{2} Z_t [v_A(t + \Delta t_{ac}) - v_A(t - \Delta t_{ac})] \\ v_C(t) &= \frac{1}{2} [v_A(t + \Delta t_{ac}) + v_A(t - \Delta t_{ac})] \\ &\quad + \left(\frac{E_t A_t}{2 Z_t} \right) [\varepsilon_A(t + \Delta t_{ac}) - \varepsilon_A(t - \Delta t_{ac})] \end{aligned} \quad (2)$$

where E_t , A_t and Z_t are respectively the elastic modulus, cross section et celerity of the tip respectively. In the Fig. 1, the measurement principle is presented, and an example of measurements process is show. Signals recorded at point A (point 1), decoupling waves (point 2) and velocity, displacement (point 3) and stress (point 4) signals reconstructed at cone/soil interface.

3.3. The DCLT curve – Analysis

By convention, the total force $F_C(t)$ for each blow is represented as a function of displacement $s_C(t)$, and this is referred to as the dynamic DCLT curve. An example of several DCLT curves obtained in field are presented in the Fig. 2.

In a first approach, to analyze DCLT curves, (Benz et al., 2013; Benz Navarrete et al., 2021) propose to model the cone-soil interaction by mean of a perfect visco elasto-platic model, as commonly proposed for pile driving problems (Smith, 1960). An analytical methodology – similar to that used for dynamic load test of piles [has been implemented in order to establish, from DCLT curves, different parameters: dynamic ($q_{d,w}$) and pseudostatic ($q_{s,w}$) cone resistance, reloading ($E_{r,w}$) and unloading modulus ($Ed_{,w}$).

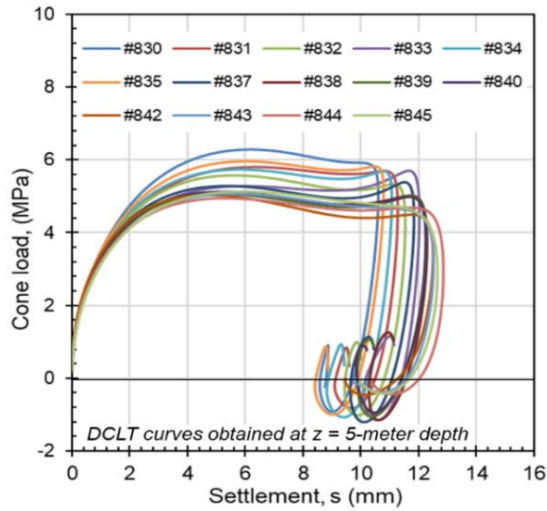


Figure 2. Example of dynamic load penetration curve (DCLT), superimposed on each other, obtained in situ at 5 meter depth.

In addition, the authors implement the shock polar method (Aussedat, 1970) to calculate compression ($V_{p,w}$) and shear wave ($V_{s,w}$) from the computed cone/soil signals $F_C(t)$ and $V_C(t)$ (Benz Navarrete et al., 2021; Oliveira et al., 2020; Teyssier et al., 2020). However, in this method, which is time domain dependent, any lag or shift in the measurement can influence the results, particularly when deeper tests are analyzed.

3.4. FRF analysis

Recently, (Tran et al., 2019) propose an alternative more reliable approach, based on FRF functions (Davis & Guillermain, 1979). FRF is a transfer function expressed in the frequency domain and it allows the spectral response of conical tip signals (acceleration, velocity, and displacement) to be analyzed as a function of the input or imposed load (force/strength). By normalizing the output signals with respect to the input signal, the characteristics, and the response of the dynamic penetrometer system, such as *accelerance*, *mechanical impedance (or mobility)* and *dynamic stiffness*, can be determined.

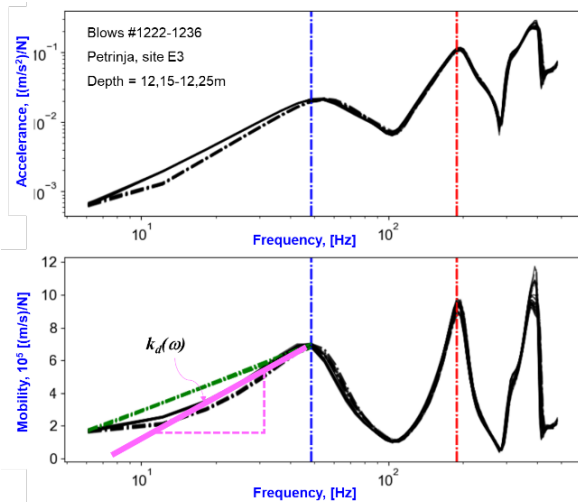


Figure 3. Example of FRF functions : Accelerance (top) and Mobility (bottom) obtained in-situ at 12 meter depth.

The FRF known as "dynamic stiffness" $k_d(\omega)$ is calculated from *mechanical impedance* by considering the strength $F_C(\omega)$ as the input load and the penetration $s_C(\omega)$ as the output response (**Eq.2**)

$$k_d(\omega) = \frac{2\pi\omega F_C(\omega)}{V_C(\omega)} \quad (1)$$

ω , $V_C(\omega)$ and $F_C(\omega)$ are the frequency, velocity and force spectrum respectively. If we consider a homogeneous elastic penetrometer of known geometry, when the frequency approaches to 0~Hz, the dynamic stiffness $k_d(\omega)$ approaches the static stiffness (k_s). However, in practice, the frequency of the dynamic impulse cannot be 0 Hz and a coefficient α representing the ratio between $k_d(\omega)$ and k_s , is introduced, where $1.5 < \alpha < 3.0$ (Davis & Guillermain, 1979).

3.5. Cone/soil or base penetrometer model

The cone/ground interaction or base penetrometer reaction can be assumed dynamically as follows:

$$Q_C(t) = ma_c(t) + C_b v_c(t) + k_b s(t) \quad (2)$$

where $Q_C(t)$, m , C_b and k_b are respectively: total strength, dynamic mass, damping and dynamic stiffness. Several cone/soil models can be applied at the base of the penetrometer to compute $Q_C(t)$, with most of them derived from pile-driving. In a first approach, (Benz Navarrete et al., 2021; Benz-Navarrete, 2009) proposes the Smith model. This is a simple linear visco elasto-plastic model that is limited to obtaining soil parameters by inverse analysis (El Naggar & Novak, 1994; Gazetas & Makris, 1991; Novak, 1991; Salgado et al., 2015). In fact, the cone soil-base model can be represented by the approach proposed by (Holeyman, 1984; El Naggar and Novak, 1994). Soil stiffness can be explained as:

$$k_s = \frac{4G_s R_H}{(1 - \nu_s)} \quad (2)$$

Moreover, it can be written

$$V_s^2 \rho_s = G_s = \frac{k_s(1 - \nu_s)}{4R_H} \quad (3)$$

where G_s is the soil shear modulus, R_H is the equivalent radius of conical model below the tip, ν_s is the soil Poisson's ratio ($\nu_s \sim 0.33$), V_s is the shear wave velocity, and ρ_s is the soil density (considered ~ 1800 kg/m³). In practice, for each blow performed and recorded during instrumented DCP driving, dynamic stiffness $k_d(\omega)$ is automatically computed from FRF curves. Assuming $\alpha = 2.5$ and solving Eq. 2 and Eq. 3, shear wave velocity V_s can be also established.

(**Fig. 4**) is an example of the results obtained at the end of a test using instrumented dynamic cone penetrometers. In the figure, cone resistance qd (obtained through the Dutch formula), dynamic $q_{d,w}$ and pseudo-static $q_{s,w}$ cone resistance obtained through signal analysis, the dynamic stiffness k_d , (**Eq. 2**), shear wave velocity $V_{s,w}$, (**Eq. 3**) and the shear modulus G for the tested soil is presented. The energy transmitted (EFV) to the penetrometer for each impact is also displayed.

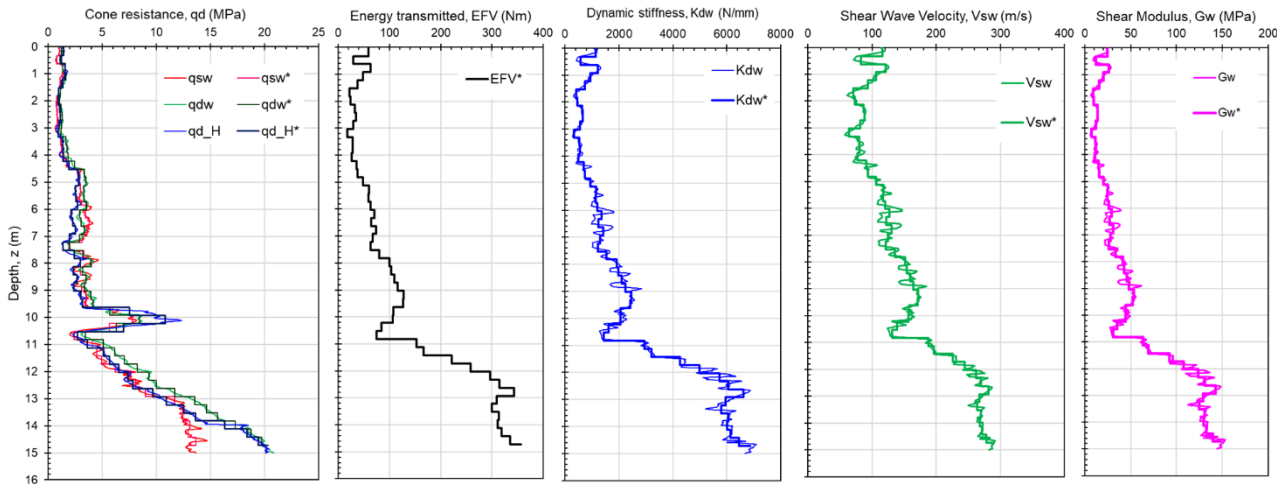


Figure 4. Example of curves Instrumented lightweight dynamic penetrometer Panda 3 – Main principle

3.6. Instruments and instrumentation

3.6.1. The Panda 3 – Lightweight iLDCP

iLDCP is composed of 6 main elements: hammer, instrumented anvil, rods, conical tips, central acquisition unit (UCA) and android tablet (HMI-Human Machine Interface) (Fig. 1). The section of the cones used is 4cm² to minimize skin friction along the rods during testing.

The UCA is an electronic data acquisition (DAQ) device designed to control and centralize information and recordings from various sensors. It processes this data before wirelessly transmitting it to a tablet computer, where an application is used for interaction with the device. The main characteristics of both the sensors and the acquisition system UCA are presented in Table 1. The total weight of the device is less than 20kg (including 5 meter of rods), which makes it easily transportable and easy to handle. Table 1 presents the main characteristics of the penetrometer.

3.6.2. The Grizzly 3 EV – Servo assisted iDPSH

iDPSH is an instrumented computer-servo-assisted, tracked penetrometer DPSH (Fig. 5).

Table 1. Main features of dynamic penetrometers

Instrumentation & DAQ characteristics		
Component	Value	
Accelerometer (g's) (x 2)	20,000 g	
Strain gage (N) (x 2)	45,000 N	
Displacement (mm)	0,1mm	
Samp. rate (Hz)	500000	
Samp. resolution (bits)	24 bits	
Record time/blow (msec)	200 msec	
Penetrometers features		
	iLDCP	iDPSH-EV
Driving system	Manual	Automatic
Type of energy	Kinetic	Potential
Hammer weight (kg)	1,726 Kg	63,5
Penetrometer weight (kg)	3.5	500
Rod length, L _R (m)	0.5	1
Rod weight, W _R (kg/ml)	1.16	5.98
Rod diameter, D _R (mm)	14	32
Cone diameter, D _c (mm)	22,6	50,5
Cone section, A _c (cm ²)	4	20
Report R _c /R _D	1,61	1,58
Cone apex angle, α(°)	90	90
Penetration power (J/cm ²)	0,2 to 28	2.5 to 23.7
Max depth (m)	< 15	< 30

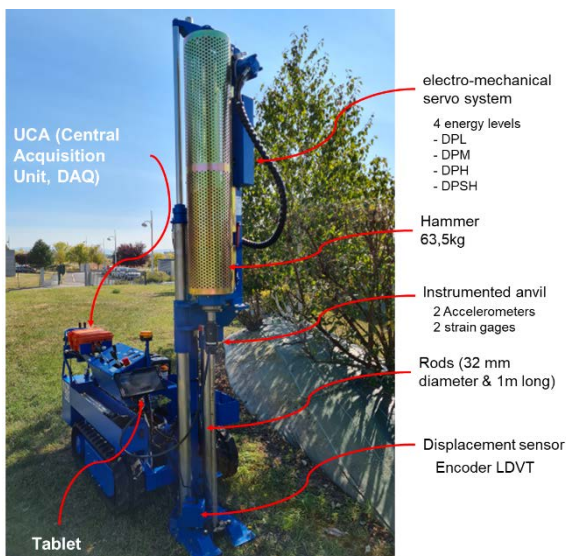


Figure 5. Servo assisted iDPSH (the Grizzly-3-EV)

The main characteristics of the device are summarized in Table 1. The test principle, instrumentation, and measurements are the same as those for the iLDCP. Nevertheless, to enhance the quality and reliability of DCLT curves obtained in soft soils (where 473 drive energy is excessive), it was necessary to devise a way to automatically adjust the drive energy in these cases, without requiring any operator intervention.

The main improvement and innovation incorporated into iDPSH is the servo-assistance assembly. This assembly comprises an electromechanical system and sensors installed on the penetrometer mast to automatically change the drive energies according to ISO 22476-2. The computer adjusts the driving energy for each blow by modifying the drop height of the hammer based on the penetration measured for the previous blow. This ensures the maintenance of a constant energy/settlement ratio throughout the test and maintain a balance between plastic and elastic settlement per blow.

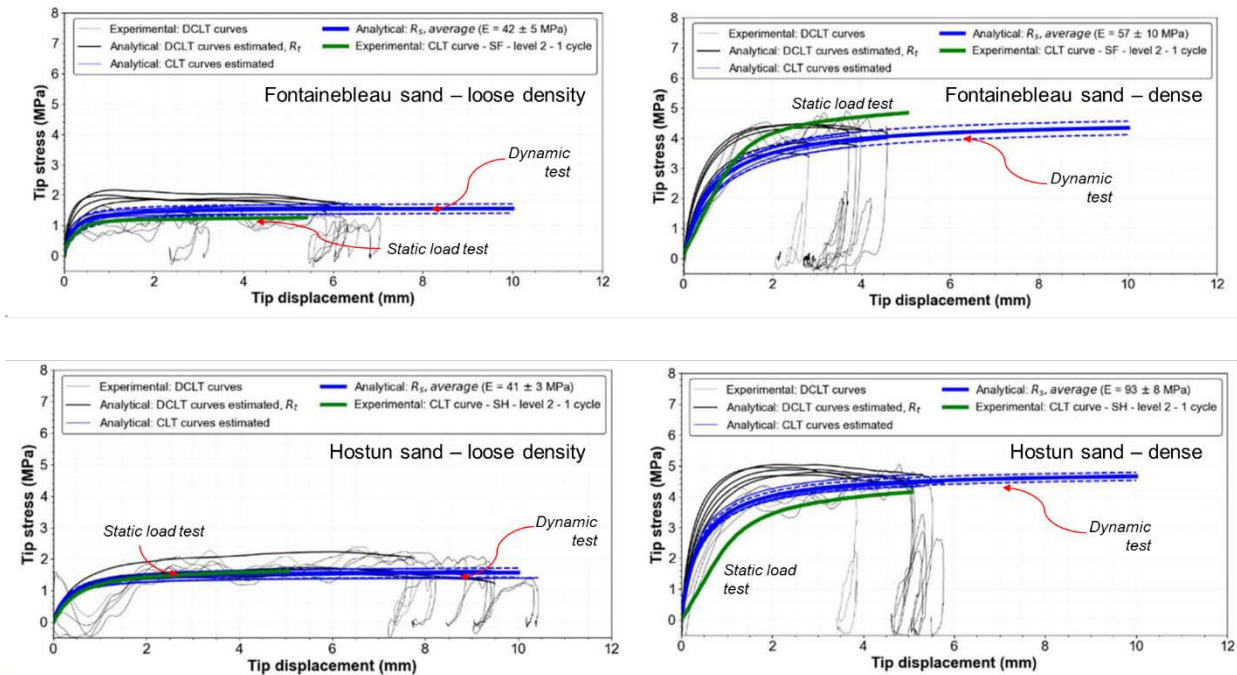


Figure 6. Petrinja, Croatia. Comparison of the shear wave velocity V_s obtained using the DCP instrument and MASW.

4. Laboratory and field test

The development of new equipment encompasses not only the assembly of the test apparatus itself but also preliminary opportunity and feasibility studies, proposals for operating procedures, laboratory and in-situ validation, and the development of an approach that allows us to derive data from test results for use in geotechnical problems.

4.1. Static and dynamic load test

A series of dynamic (iLDCP) and static (CLT) penetrometric cone loading tests were carried out in the laboratory. The aim of these tests was to compare the curves obtained using the two techniques and to assess the relevance of the DCLT curves. The soils studied were Hostun sand HN31 (SH) and Fontainebleau sand NE34 (SF). Each sample tested was reconstituted to two different density states in a metal calibration chamber 372 mm in diameter and 805 mm high. The boundary conditions were as follows: displacements prevented radially and zero vertical stress at the surface (type BC3 chamber).

Loading tests were conducted along the axis of the specimen. The penetrometer was manually driven to various depths, and each impact was recorded to obtain a DCLT curve. Once the required depth was reached, the driving was stopped, and the CLT test was carried out at a constant rate (0.01 mm/s).

Fig. 6 shows the results obtained. In general, the DCLT and CLT curves exhibit good repeatability and agreement. Similar orders of magnitude can be observed for the stresses in the curves produced by these two techniques.

4.2. Density index and overburden pressure

As part of the studies conducted to propose a methodology for analyzing liquefaction risk assessment of sandy soils using instrumented penetration tests, a series of tests were performed on sand (Fontainebleau and Hostun) samples in calibration chamber. For each sand, different samples were made by varying the density index, with the confining pressure adjusted for each specimen -10, 20, 50, 75, 100, 200, 300, 400 Kpa).

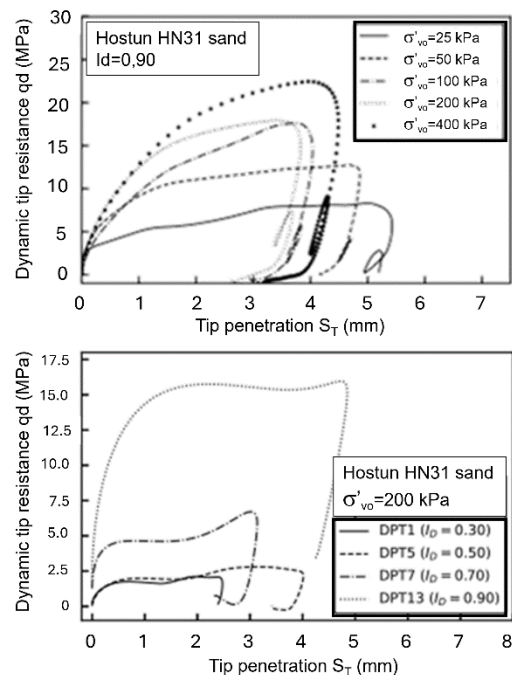


Figure 7. DCLT curves obtained in laboratory, in a calibration chamber, for Hostun sand. Effects of vertical pressure (top) and index of density (bottom).

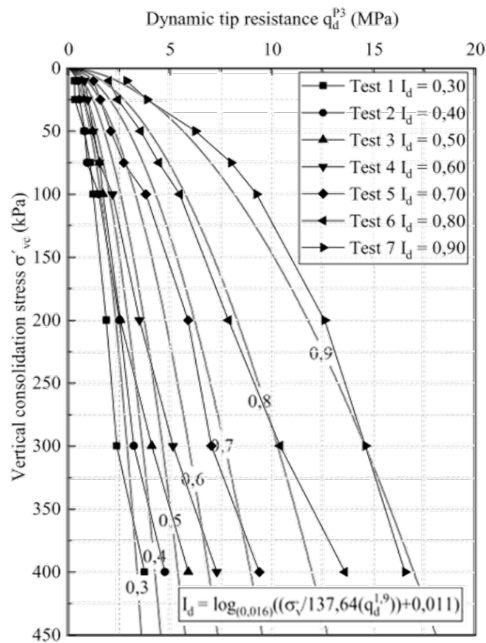


Figure 8. Vertical stress, index of density and cone resistance q_d relationship.

On each sample, a dynamic penetration test was conducted and for each hammer blow, strain, forces, acceleration, displacement, DCLT curves and cone resistance profiles were recorded. At the end, graphs, or charts for correlating q_d , density index and overburden pressure.

Fig. 7 illustrates an example of the DCLT curves obtained for Hostun sand at various densities and different vertical stresses. DCLT curves are sensitive to changes in the state of the specimens tested. At the conclusion of the tests, we can establish a correlation between the index of density, the confining pressure, and the measured cone resistance q_d .

Figure 8 illustrates this formulation based on laboratory results obtained for dry sands (Hostun and Fontainebleau), with a density index variation ranging between 0.3 and 0.9.

4.3. Shear wave velocity assessment.

The soil shear wave velocity (V_s) is one of the key features in studying soil behavior under cyclic stresses like earthquakes. The shear wave velocity is today the reference parameter for soil classification under seismic stresses as well as for the study of the risk of liquefaction on structures. Various comparative tests using instrumented DCP, have been carried out and presented in the past (Teyssier et al., 2020; Tran et al., 2019).

More recently, as part of missions to study the Paleo liquefaction of sandy soils, iDPSH tests in addition to MASW were carried out in Croatia, on an area that had experimented liquefaction during the Mw 6.4 Petrinja earthquake on the 29th December 2020.

In fact, to evaluate the relevance of the measurements carried out, we compared them with measurements performed with MASW available for each site. In addition, we are interested in assessing the complementarity of these two techniques, which would improve the vertical resolution of measurements taken with surface seismic methods. Fig. 9 shows the results obtained using both methods (instrumented DCP and MASW) at the Petrinja. At the three sites studied and presented at Petrinja (Fig. 9), the measurement of V_s shows a good agreement, both in terms of vertical evolution and amplitude. However, and assuming no errors in MASW interpretation, it can be observed that the V_s values on the surface ($0 < z < 4$ m) are generally lower than those deduced from the MASW tests, mainly for D1 and D2 site. A good agreement between both methods was obtained in site E1.

Acknowledgements

The authors are grateful for the financial support provided by the FUI-24 EmerG3r project, as well as its academic (Université Gustave Eiffel et Ecole des Ponts Paris Tech, Université Blaise Pascal) and industrial (Sol Solution, Fondasol and CIO systems) partners who have made all this work possible.

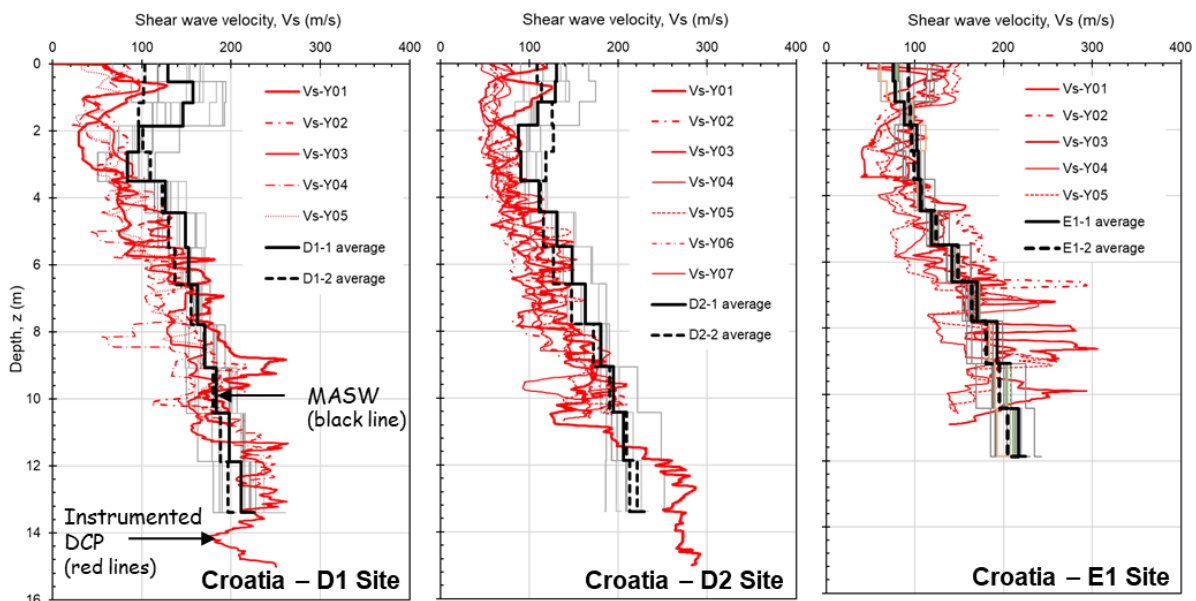


Figure 9. Petrinja, Croatia. Comparison of the shear wave velocity V_s obtained using the DCP instrument and MASW.

5. Conclusions

Dynamic penetration test are widely used around the world and currently provide a single failure parameter, the cone resistance q_d . However, its technical and technological development have remained in most cases a, rudimentary. In this work, based on the works carried out on the French variable energy penetrometer, (The Panda), a lightweight dynamic variable energy penetrometer and a super heavy DPSH has been instrumented to measure the strain $\epsilon(x, t)$, acceleration $a(x, t)$ and displacement $s(t)$ variations caused within the rods by the compressional wave created immediately after each hammer blow and during penetrometer driving. By using a wave decoupling and reconstruction method, it has been possible to directly obtain the DCLT curve of the soil at each blow. As demonstrated by a series of tests, the resulting DCLT curve is reproducible, sensitive, and reliable to the test conditions as well as to the soil conditions. The technical feasibility of the method as well as the reliability of the results has been proved in situ by a series of tests with continuous recordings up to a depth of 7 m.

This work has revived interest in the dynamic penetrometer technique for shallow soil characterization, particularly the instrumented variable energy driving penetrometer. It is proving to be a valuable tool for various cases encountered in practice, and the results obtained complement those of other techniques such as CPT, MASW, and SPT. As for other equipment, dynamic penetrometers must, by default, measure the energy transferred to the rod during the test.

References

Aussedat, G. (1970). Sollicitations rapides des sols. University of Grenoble, France.

Barré de Saint-Venant, J. C. (1867). Mémoire sur le choc longitudinal de deux barres élastiques de grosseurs et de matières semblables ou différentes ... *Journal Des Mathématiques Pures et Appliquées*, 2(XII), 237–376.

Benz, M. A., Escobar, E., Gourvès, R., Haddani, Y., Breul, P., & Bacconnet, C. (2013). Dynamic measurements of the penetration test - Determination of the tip's dynamic load-penetration curve. 18th International Conference on Soil Mechanics and Geotechnical Engineering: Challenges and Innovations in Geotechnics, ICSMGE 2013, 1.

Benz Navarrete, M. A., Breul, P., & Gourvès, R. (2021). Application of wave equation theory to improve dynamic cone penetration test for shallow soil characterisation. *Journal of Rock Mechanics and Geotechnical Engineering*. <https://doi.org/10.1016/j.jrmge.2021.07.004>

Benz Navarrete, M. A., Breul, P., & Moustan, P. (2019). Servo-Assisted and Computer-Controlled Variable Energy Dynamic Super Heavy Penetrometer. *Geotechnical Engineering in the XXI Century: Lessons Learned and Future Challenges*, 0, 65–72. <https://doi.org/10.3233/STAL190024>

Benz-Navarrete, M. A. (2009). Mesures dynamiques lors du battage du pénétromètre Panda 2.

Broms, B., & Flodin, F. (1988). History of soil penetration testing. *Proceedings ISOPT1, Orlando, U.S.A.*, 1, 157–220.

Byun, Y.-H., & Lee, J.-S. (2013). Instrumented Dynamic Cone Penetrometer Corrected with Transferred Energy into a Cone

Tip: A Laboratory Study. *Geotechnical Testing Journal*, 36. <https://doi.org/10.1520/GTJ20120115>

CEN. (2007). EN 1997-2 - Eurocode 7 : Calcul géotechnique Partie 2 : Reconnaissance des terrains et essais (Vol. 33).

Davis, A., & Guillermain, P. (1979). Interprétation géotechnique des courbes de réponse de l'excitation harmonique d'un pieu. *Revue Française de Géotechnique*, 8, 15–21. <https://doi.org/10.1051/geotech/1979008015>

DeJong, J. T., Ghafghazi, M., Sturm, A. P., Wilson, D. W., den Dulk, J., Armstrong, R. J., Perez, A., & Davis, C. A. (2017). Instrumented Becker Penetration Test. I: Equipment, Operation, and Performance. *Journal of Geotechnical and Geoenvironmental Engineering*, 143(9). [https://doi.org/10.1061/\(asce\)gt.1943-5606.0001717](https://doi.org/10.1061/(asce)gt.1943-5606.0001717)

El Naggar, M. H., & Novak, M. (1994). Non-Linear Model for Dynamic Axial Pile Response. *Journal of Geotechnical Engineering*, 120(2), 308–329. [https://doi.org/https://doi.org/10.1061/\(ASCE\)0733-9410\(1994\)120:2\(308\)](https://doi.org/https://doi.org/10.1061/(ASCE)0733-9410(1994)120:2(308))

Escobar Valencia, E. J., Benz Navarrete, M. A., Gourvès, R., Breul, P., & Chevalier, B. (2016). Le Grizzly 3 à énergie variable : Nouveaux développements de l'essai de pénétration dynamique. *Journées Nationales de Géotechnique et de Géologie de l'Ingénieur, JNGG 2016*, 1–8.

Fairhurst, C. (1959). Energy Transmission in Percussive drilling. *Journal of Petroleum Technology*, 11. <https://doi.org/https://doi.org/10.2118/1287-G>

Gazetas, G., & Makris, N. (1991). Dynamic pile-soil-pile interaction. Part I: Analysis of axial vibration. *Earthquake Engineering & Structural Dynamics*, 20(2), 115–132. <https://doi.org/https://doi.org/10.1002/eqe.4290200203>

Goldmann, N. (1699). *Comprehensive guidelines to the art of building (Vollständige Anweisung zu der Civil Bau-Kunst)*.

Gourvès, R. (1991). Le PANDA : pénétromètre dynamique léger à énergie variable pour la reconnaissance des sols.

Gourvès, R., & Barjot, R. (1995). Le pénétromètre dynamique léger PANDA. 11ème Congrès Européens de Mécanique Des Sols et Des Travaux de Fondations, 83–88.

ISO-22476-2. (2005). Reconnaissance et essais géotechniques — Essais en place — Partie 2: Essais de pénétration dynamique.

Khalaf, K., & Briaud, J. L. (1992). Driven Cone Penetrometer for Pile Driving Analysis. <https://hdl.handle.net/1969.1/ETD-TAMU-1992-THESIS-K446>

Kianirad, E. (2011). Development and Testing of a Portable In-Situ Near-Surface Soil Characterization System. Northeastern University.

Liang, R. Y., & Sheng, Y. (1993). Wave Equation Parameters from Driven-Rod Test. *Journal of Geotechnical Engineering*, 119(6), 1037–1057.

Matsumoto, T., Phan, L. T., Oshima, A., & Shimono, S. (2015). Measurements of driving energy in SPT and various dynamic cone penetration tests. *Soils and Foundations*, 55(1), 201–212. <https://doi.org/10.1016/j.sandf.2014.12.016>

Nazarian, S., Tandom, V., Crain, K., & Yuan, D. (1998). Feasibility Study on Improvements to Dynamic Cone Penetrometer.

Novak, M. (1991). Piles under dynamic loads. *Proceedings: Second International Conference on Recent Advances in Geotechnical Earthquake Engineering and Soil Dynamics*, 1974, 2433–2456.

Oliveira, C. F., Navarrete, M. A. B., Tran, Q. A., Breul, P., Chevalier, B., & Bacconnet, C. (2020). Assessment of small-strain modulus through wave velocity measurement with dynamic penetrometer Panda 3@. 6th International Conference on Geotechnical and Geophysical Site Characterization (ISC).

Sabtan, A. A., & Shehata, W. M. (1994). Le pénétromètre mackintosh utilisé comme outil de reconnaissance. *Bulletin of the International Association of Engineering Geology - Bulletin*

de l'Association Internationale de Géologie de l'Ingénieur, 50(1), 89–94. <https://doi.org/10.1007/BF02594960>

Salgado, R., Loukidis, D., Abou-Jaoude, G., & Zhang, Y. (2015). The role of soil stiffness non-linearity in 1D pile driving simulations. *Géotechnique*, 65(3), 169–187. <https://doi.org/10.1680/geot.13.p.124>

Salgado, R., & Yoon, S. (2003). Dynamic Cone Penetration Test (DCPT) for Subgrade Assessment (Issue February). <https://docs.lib.purdue.edu/cgi/viewcontent.cgi?article=1544&context=jtrp>

Sanglerat, G. (1972). The penetrometer and soil exploration. Interpretation of penetration diagrams — Theory and practice. In Elsevier Publishing Company. ELSEVIER PUBLISHING COMPANY. [https://doi.org/10.1016/0012-8252\(73\)90164-5](https://doi.org/10.1016/0012-8252(73)90164-5)

Scala, A. J. (1956). Simple methods of flexible pavement design using cone penetrometers. Australia New Zealand Conference On Soil Mechanics and Foundation Engineering, 33–44.

Schmertmann, J. H. (1978). Use the SPT to Measure Dynamic Soil Properties?—Yes, But..! In ASTM (Ed.), STP654 Dynamic Geotechnical Testing (pp. 341–355). ASTM. <https://doi.org/10.1520/STP35685S>

Schmertmann, J. H., & Palacios, A. (1979). Energy Dynamics of SPT. *Journal of the Geotechnical Engineering Division*, 105(8), 909–926.

Smith, E. A. L. (1960). Pile-driving analysis by the wave equation. *Journal of the Soil Mechanics and Foundations Division*, 86(4).

Sowers, G., & Hedges, C. (1966). Dynamic Cone for Shallow In-Situ Penetration Testing. In ASTM (Ed.), Vane Shear and Cone Penetration Resistance Testing of In-Situ Soils, (p. 29). <https://doi.org/10.1520/STP44629S>

Teyssier, A., Navarrete, M. A. B., TRAN, Q. A., Péllez, J. C., & Jacquard, C. (2020). Field correlation between shear wave velocity measured by Panda 3@ , Ménard pressuremeter test (PMT), cone penetration test (CPT) and geophysical tests. 6th International Conference on Geotechnical and Geophysical Site Characterization, 406(2).

Tran, Q. A., Benz Navarrete, M. A., Breul, P., Chevalier, B., & Moustan, P. (2019). Soil dynamic stiffness and wave velocity measurement through dynamic cone penetrometer and wave analysis. *Geotechnical Engineering in the XXI Century: Lessons Learned and Future Challenges* N.P. López-Acosta et al. (Eds.), 1, 1–8. <https://doi.org/10.3233/STAL190064>

Webster, S. L., Grau, R. H., & Williams, T. P. (1992). Description and Application of Dual Mass Dynamic Cone Penetrometer.

